한국기계가공학회지, 제19권, 제1호, pp.100～107(2020.01) ISSN 1598-6721(Print)
Journal of the Korean Society of Manufacturing Process Engineers, Vol. 19, No. 1, pp.100~107(2020.01) ISSN 2288-0771(Online)

https://doi.org/10.14775/ksmpe.2020.19.01.100

An Analytical Study on the Thermal-Structure Stability Evaluation of Mill-Turn Spindle with Curvic Coupling

Choon-Man Lee*,#, Ho-In Jeong**
*Dept. of Mechanical Engineering, College of Mechatronics, Changwon National University,
**Mechanical Design and Manufacturing, School of Mechatronics Engineering, Changwon National University

커빅 커플링을 적용한 밀-턴 스핀들의 열-구조 안정성 평가에 관한 해석적 연구

이춘만*,#, 정호인**
*창원대학교 기계공학부, **창원대학교 메카트로닉스공학부

(Received 18 November 2019; received in revised form 30 November 2019; accepted 19 December 2019)

ABSTRACT

As demand for high value-added products with hard materials increases, the line center is used for producing high value-added products in many industries such as aerospace, automobile fields. The line center is a key device for smart factory automation that can improve the production efficiency and the productivity. Therefore, the development of a mill-turn line center is necessary to produce high value-added products with complex shapes flexibly. In the mill-turn process, a milling process and a turning process are combined. In particular, the turning process needs to increase the rigidity of the spindle. The purpose of this study is to analyze the thermal-structural stability through thermo-structural coupled analysis for a mill-turn spindle with a curvic coupling. The maximum temperature and thermal stability of the spindle were analyzed by thermal distribution. In addition, the thermal deformation and thermal-structural stability of the spindle were analyzed through thermo-structural coupled analysis.

Key Words : Spindle(스핀들), Mill-turn Process(밀-턴 가공), Curvic Coupling(커빅 커플링), Thermal-structure Stability(열-구조 안정성), Thermal-structure Coupled Analysis(열-구조 연성해석)

1. Introduction

Today, interest in high value-added industries including the global automotive market have risen, and emerging economies such as China, India, and other ASEAN countries are investing in factory facilities to produce high value-added products. In particular, these countries are importing compact and excellent performance line centers and are using them as core equipment in production lines. In South Korea, line centers for producing automotive parts are rarely developed domestically; instead, products from leading companies are imported. Furthermore, to satisfy the latest collision safety laws in the automotive industry, high-strength

Corresponding Author : cmlee@changwon.ac.kr
Tel: +82-55-213-3622, Fax: +82-55-267-1160

composite materials such as carbon fiber reinforced plastics (CFRP) that can simultaneously satisfy requirements for lightness in weight and safety are being increasingly used. Consequently, mill-turn machining, which combines the existing milling with turning, is required to increase spindle stiffness [1–4]. Therefore, the domestic development of a compact mill-turn line center to produce high value-added products such as automobiles and aviation parts with complex shapes is required.

This study used thermal analysis to contribute to thermal stabilization designs before producing a mill-turn spindle that can perform machining at a high speed, stiffness, and precision using Curvic Coupling. The precision of high-speed machining is greatly affected by thermal strain. Therefore, before developing the spindle, the thermal characteristics were analyzed through thermal analysis. For spindle thermal analysis, the bearing heating value at the maximum spindle speed was calculated and used as the heat source, and thermal analysis was performed considering the cooling effects of the cooling jacket in the ball bearing and built-in motor. After analyzing the temperature maximum and distribution of the spindle through thermal analysis, the thermal-structural stability of the spindle was analyzed according to the thermal displacement and Curvic Coupling motions of the spindle through thermal-structural coupled analysis. The mill-turn spindle to be developed is fixed to both ends of the shaft using double-row ceramic ball bearings of the DT combination for high-speed and high-stiffness machining. The spindle stiffness was increased by changing the preload according to the rotation speed of the mill-turn spindle by applying a variable preload system [5].

2. Structure of Mill-turn Spindle

The mill-turn spindle with curvic coupling has a structure that increases the stiffness of the spindle shaft by fastening the Curvic Coupling during turning. The motor of the mill-turn spindle is built in the housing, and either end of the shaft is supported by a double-row ceramic ball bearing. The rear wheel bearing part has a variable preload system that applies a light preload when the mill-turn spindle rotates at a low speed and a heavy preload when it rotates at a high speed to increase the mill-turn spindle's stiffness. Furthermore, spindle heating is suppressed by designing a cooling jacket in the spindle housing to cool the bearing and motor, which are main causes of heating during spindle operation. Fig. 1 shows the structure of the mill-turn spindle used in this study.

The Curvic Coupling is mounted on the back. It is decoupled during milling and one part rotates together with the shaft and the other part is fixed to the housing. During turning, the part fixed to the

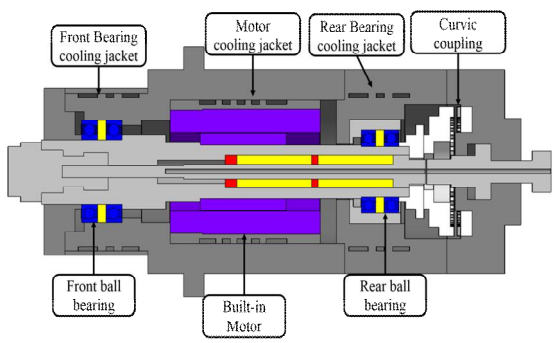

Fig. 1 3D model of the mill-turn spindle

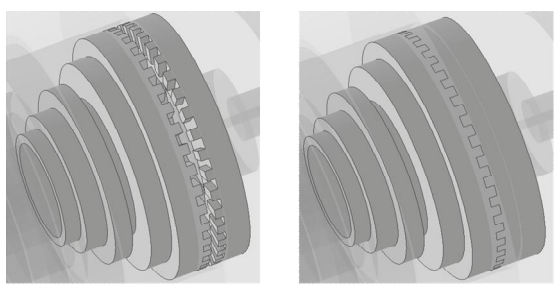

(a) Position at the milling process (b) Position at the turning process

Fig. 2 The curvic coupling position according to machining methods

housing is moved by external hydraulic pressure and coupled with the part fixed to the shaft. The coupled coupling is fixed by hydraulic pressured and increases the stiffness of the shaft by fixing the shaft. Fig. 2 shows the location of the Curvic Coupling during milling and turning.

3. Thermal Analysis

3.1 Analysis model and boundary conditions

Before performing the thermal-structural coupled analysis, we performed thermal analysis to analyze the temperature distribution of the spindle according to the operation conditions of the mill-turn spindle. The maximum rotation speed of the spindle during milling is 20,000 rpm, and it is 1,000 rpm during turning. Because the rotation speed during turning is slow, thermal analysis was performed only under the milling condition. The mesh analysis model was composed of 435,909 nodes and 110,028 elements by configuring the grids using the hex dominant (Quad/Tri) and sweep methods. Fig. 3 shows the analysis model used. The materials used were SM45C, SCM415, and SUJ2. Furthermore, SCM415 was applied to rotating bodies such as the shaft and drawbar, SUJ2 was applied to the bearings, and SM45C was applied to parts such as the spindle housing. Table 1 lists the properties of each material. Regarding the boundary conditions for

Table 1 Mechanical properties of material

	SM45C	SCM415	SUJ2
Density(kg/m^3)	7,850	7,700	7,810
Young's modulus(GPa)	205	190	210
Poisson's ratio	0.29	0.27	0.30
Tensile yield strength(MPa)	343	415	120
Thermal conductivity(W/m-℃)	49.8	42.6	46.6

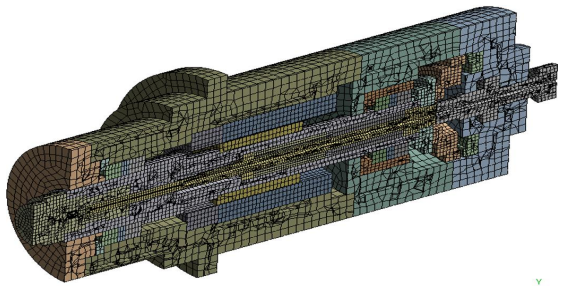

Fig. 3 Analysis model of the mill-turn spindle

analysis, the heating, cooling, and heat transfer characteristics of the spindle were calculated, and the calculation results were applied.

3.2 Bearing heating characteristics

The maximum rotation speed of the mill-turn spindle was 20,000 rpm. Ceramic ball bearings were used to reduce the bearing heat resulting from high-speed rotation. Ceramic balls have a higher stiffness and lower heat generation than bearing steel. Therefore, we adopted bearings using ceramic materials for rolling elements.

Since bearing heat is generated by friction loss in the rotational movement, we calculated the heating value ($H_{bearing}$) of the bearing by obtaining the friction moment (M_{total}). The heating value was determined using the Palmgren formula, which is divided into two parts: the viscous moment term ($M_{viscousity}$), which determines the friction moment according to the lubricant and bearing speed, and the load moment term (M_{load}) by load. The viscous moment term is calculated using the bearing viscosity coefficient (f_0), pitch diameter of bearing (d_m), kinematic viscosity of lubricant (ν), and number of revolutions per bearing (n). The friction moment term is calculated using the load coefficient of bearing (f_1), the equivalent load of bearing (P_1), and the pitch diameter of bearing. For the bearing coefficient and kinematic viscosity of lubricant, the data provided by each manufacturer was applied[6–7].

$$M_{total} = M_{viscosity} + M_{load} \quad (1)$$

$$M_{viscousity} = f_0 \cdot 10^{-7} \cdot {d_m}^3 \cdot (\nu \cdot n)^{2/3} \quad (2)$$

$$M_{load} = f_1 \cdot P_1 \cdot d_m \quad (3)$$

$$H_{bearing} = \frac{2\pi}{60} \cdot 10^{-3} \cdot n \cdot M_{total} \quad (4)$$

3.3 Heating characteristics of the embedded motor

For the embedded motor used in the spindle system, the SIMOTICS M-1FE1 model of SIEMESNS was used. The motor heating value was calculated using the output-torque diagram and heating data provided by the manufacturer. Fig. 4 shows the output-torque diagram of the built-in motor [8].

3.4 Cooling characteristics of the cooling jacket

The cooling oil that flows along the cooling jacket and cools down the built-in motor and bearing was assumed to be a fluid that flows inside a rectangular pipe. The cooling capacity was calculated by introducing the hydraulic diameter

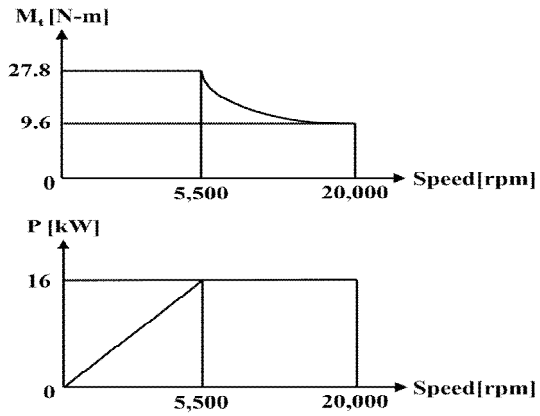

Fig. 4 Output-torque diagram of the built-in motor

(d_h). The hydraulic diameter was calculated by the cross-sectional area (A) and perimeter (P) of the pipe.

$$d_h = \frac{4 \cdot A}{P} \quad (4)$$

A constant flow of 10 L/min of cooling oil was supplied to every cooling jacket, and the temperature of the cooling oil was maintained at 20ºC. To calculate the cooling capacity of the cooling jacket, its convective heat transfer coefficient ($h_{Cooling\,jaket}$) was calculated by applying the Nusselt number (Nu_{d_h}) and thermal conductivity (k_{oil}) of the cooling oil. The Nusselt number of the internal flow for the turbulent flow inside the pipe was calculated by applying the Reynolds number (Re_{d_h}), Prandtl number (Pr), and the friction coefficient of the pipe (f) [9].

$$h_{Cooling\,jaket} = \frac{k_{oil} \cdot Nu_{d_h}}{d_h} \quad (5)$$

$$Nu_{d_h} = \frac{(f/8)(Re_{d_h} - 1{,}000)\mathrm{Pr}}{1 + 12.7(f/8)^{1/2}(\mathrm{Pr}^{2/3} - 1)} \quad (6)$$

3.5 Heat transfer characteristics

The natural convective heat transfer coefficient was applied to the convective heat transfer coefficient regarding the heat transfer of the spindle surface exposed to air. The heat transfer coefficient according to the shaft rotation speed was applied to the heat transfer coefficient according to the rotation of the shaft. Fig. 5 shows the heat transfer coefficient according to the shaft rotation speed [10].

The gap between the rotor and stator of the motor is very small in thickness. Therefore, most air cannot escape to the outside of the gap, and as the rotor rotates, heat transfer occurs through the forced convection with the stator. Regarding the heat

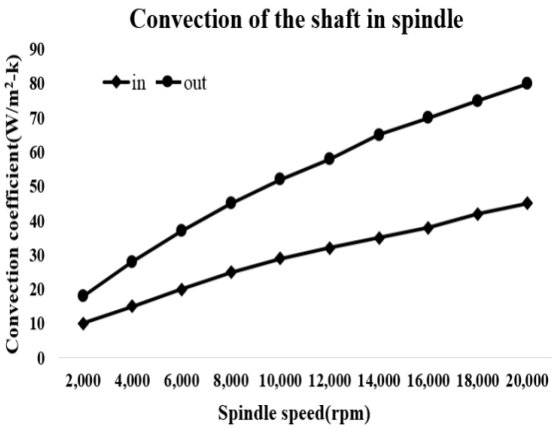

Fig. 5 Convection of the shaft in spindle

transfer characteristics of the gap between the rotor and stator, the convective heat transfer coefficient (h_{gap}) between the gaps was calculated assuming a simple plate flow with very narrow spacing. For this calculation, the Nusselt number (Nu_{d_g}) and thermal conductivity (k_{air}) of the air between the gaps was applied. The Nusselt number (Nu_{d_g}) in a simple plate flow was calculated by applying the Reynolds number (Re_{d_h}) and the Prandtl number (Pr) [11].

$$h_{Motorgap} = \frac{k \cdot Nu_{d_g}}{d_g} \tag{7}$$

$$Nu_{d_g} = 0.664 \cdot Re^{1/2} \cdot \Pr^{1/3} \tag{8}$$

3.6 Thermal analysis results

The analysis results showed that the maximum temperature of the turn spindle was 35.8℃ (in the range of 20–40 ℃, the spindle operation condition for commercial machine tools) in the front wheel bearing of the spindle. Fig. 6 shows the temperature distribution of the mill-turn spindle. Heat was found to be generated in the bearing and motor, which are the main heat sources of the mill-turn spindle;

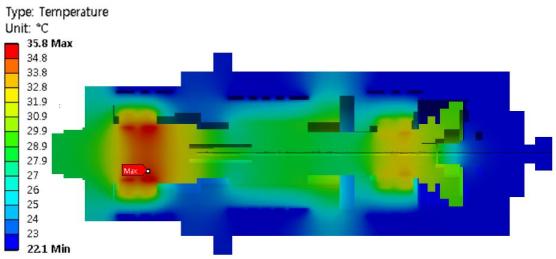

Fig. 6 Thermal distribution of the mill-turn spindle

additionally, thermal stability was achieved by with the role of the cooling jacket, which cooled the housing and maintained room temperature.

4. Thermal-structural Coupled Analysis

4.1 Spindle analysis of milling condition

For the thermal-structural coupled analysis model of the spindle in the milling condition, the same thermal analysis model was used. Regarding the boundary conditions for structural analysis, the rotation speed of the shaft was set to 20,000 rpm. Considering the tool length, the remote force condition at 50 mm from the tip of the spindle was used, and a cutting force of 1,000 N in axial direction was applied. For the cutting force, a value that can be applied to the spindle for general high-speed machining was considered [12]. Furthermore, the self-weight was considered by setting the gravity condition for the entire spindle. The effect of spindle heating was analyzed by setting the temperature obtained from the thermal analysis as the boundary condition. For structural analysis that focused on heating and thermal displacement according to the operation of the mill-turn spindle in this study, the assembled state of the mill-turn spindle was assumed as the steady state, and the bearing stiffness was not considered in this study in the performance of static analysis [13]. Fig. 7 shows the boundary conditions of the spindle during milling.

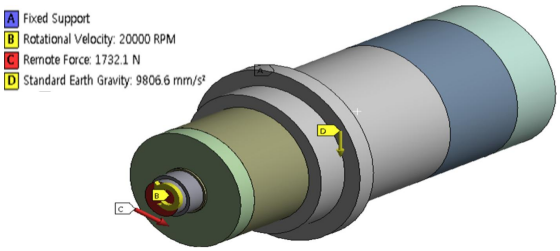

Fig. 7 Boundary conditions of the mill-turn spindle at milling process

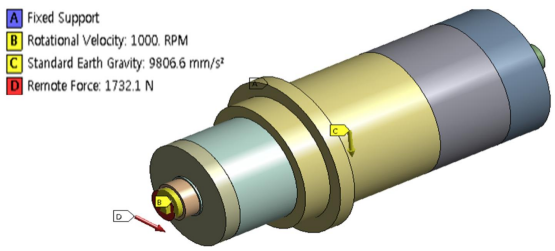

Fig. 8 Boundary conditions of the mill-turn spindle at turning process

4.2 Spindle analysis of turning condition

Thermal analysis was not performed for the turning condition because the spindle does not rotate at a high speed, and heat generation is insignificant. Structural analysis was performed to analyze the increased stiffness of the shaft due to the coupling operation. For the boundary condition, the rotation speed of the spindle was set to 1,000 rpm. As with the milling process, a cutting force of 1,000 N was applied in the axial direction at 50 mm from the spindle tip, and the self-weight was considered by applying the gravity condition to the entire spindle. Fig. 8 shows the boundary conditions of the spindle during turning.

5. Analysis Results

5.1 Spindle analysis results for the milling condition

The analysis results showed that the maximum displacement and maximum stress of the spindle in milling condition during Curvic coupling were 49.5 μm and 179 MPa, respectively. In the milling process, Curvic Coupling was decoupled and rotated at the same speed as the shaft, resulting in a large displacement and stress due to torque. The maximum strain of the shaft that actually influenced machining precision was 5.3 μm, and the safety factor of the spindle was approximately 2. Figs. 9 and 10 show the thermal-structural coupled analysis

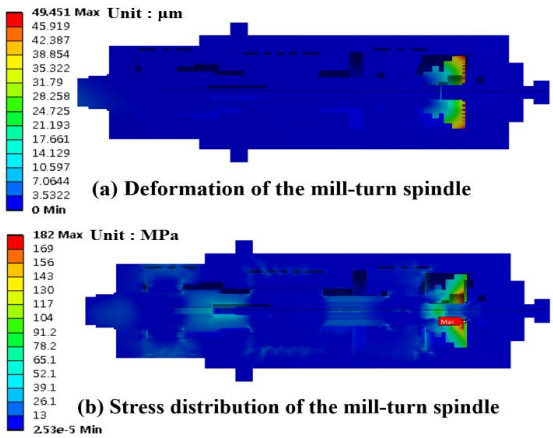

Fig. 9 Analysis results of the mill-turn spindle at milling process

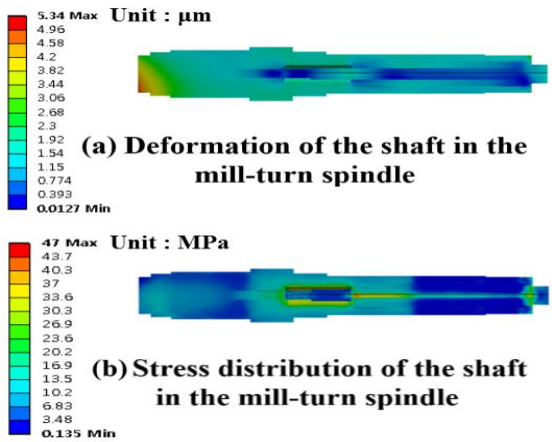

Fig. 10 Analysis results of the shaft in mill-turn spindle

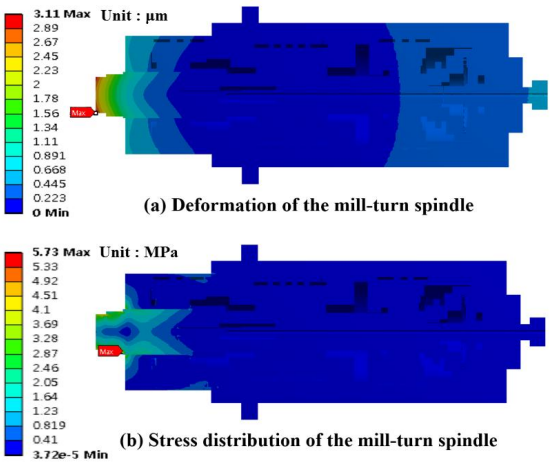

Fig. 11 Analysis results of the mill-turn spindle at turning process

results for the entire spindle and the shaft under the milling condition, respectively.

5.2 Spindle analysis results of the turning condition

The analysis result showed that the maximum displacement of the spindle in the turning condition at the spindle tip was 3.1 μm, and the maximum stress was 5.73 MPa between the shaft and the housing. During turning, the spindle stiffness increased as a result of the Curvic Coupling, and low strain and stress were generated. The safety factor was approximately 60 (safety factor was 40 during the milling process at 1,000 rpm), confirming increased spindle stiffness. Fig. 11 shows the thermal-structural coupled analysis results of the spindle in the turning condition.

6. Conclusion

In this study, the temperature maximum and distribution of a spindle were analyzed through thermal analysis before the fabrication of a high-precision mill-turn spindle that can perform at a high speed and stiffness for machining using Curvic Coupling. Then, the thermal-structural stability of the spindle according to the thermal displacement of the spindle and the operation of the Curvic Coupling were analyzed through the thermal-structural coupled analysis. The maximum temperature of the mill-turn spindle was 35.8ºC and the maximum safety factor was 60. The conclusions of this study are as follows:

1. As a result of thermal analysis by calculating the heating, cooling, and heat transfer characteristics of the spindle using the aforementioned equations, the maximum temperature of the spindle was 35.8ºC. This is lower than the proper operating temperature of commercial machine tools, thus verifying the thermal stability of the mill-turn spindle.
2. As a result of the thermal-structural coupled analysis, the maximum strain of the mill-turn spindle in the milling condition was 49.5 μm, the maximum stress was 179 MPa, and the safety factor was approximately 2.
3. A strain of 49.5 μm in the milling condition was caused by the rotation of the Curvic Coupling. The strain of the shaft that actually affects the machining precision was approximately 5.3 μm, indicating an insignificant strain.
4. The maximum strain and stress of the mill-turn spindle in the turning condition were 3.1 μm and 5.73 MPa, respectively. Thus, the spindle stiffness increased as a result of the Curvic Coupling during turning, and the safety factor of the spindle was approximately 60 (the safety factor was 40 for the milling process at 1,000 rpm), thus verifying the structural stability of the mill-turn spindle.

The results of this study will be applied to developments in the design and manufacturing of a mill-turn spindle of a compact line center for

machining complex-shaped parts.

Acknowledgements

This study was conducted with the support of the industrial technology innovation project of the Ministry of Trade, Industry and Energy (“Development of a line center with 15% or higher compact index with IoT/AI smart condition diagnosis/calibration and dual head for machining complex-shaped parts;” No. 20003806).

References

1. Lee, M. J. and Lee, C. M., "Development of Analysis Model for Geometric Error in Turning processes," Journal of Central South University, Vol. 18, pp. 711-717, 2011.
2. Choi, J. Y. and Lee, C. M., "Evaluation of Cutting force and Surface Temperature for Round and Square member in Laser Assisted Turn-Mill," Journal of Applied Mechanics and Materials, Vol. 229-231, pp. 718-722, 2012.
3. Lee, C. M. and Ahn, J. W., "Study on the Evaluation of Machining Characteristics of Trochoidal Profile by Turn-Mill," Journal of the Korean Society for Precision Engineering, Vol. 33, No. 2, pp. 95-100, 2016.
4. Lee, C. M. and Kim, E. J., "A Study on the Machining Characteristics of a Turning-Center by Laser Assisted Machining," Journal of the Korean Society for Precision Engineering, Vol. 35, No. 6, pp. 597-601, 2018.
5. Kim, D. H., Woo, W. S., Lee, C. M. and Hwang, Y. K, "Performance Evaluation of a Variable Preload Spindle by Using Linear Actuator," Journal of the Korean Society for Precision Engineering, Vol. 34, No. 8, pp. 511-515, 2017.
6. Kim, K. S., Hwang, J. H., Lee, D. W., Lee, S. M. and Lee, S. J., "Study on the Frictional Torque in the Angular Contact Ball Bearing for Machine Tool Spindle by Empirical Formula," Journal of the Korean Society for Precision Engineering, Vol. 32, No. 2, pp. 149-157, 2015.
7. Kim, J. D., Zverv, I. and Lee, K. B., "Thermal Model of High-Speed Spindle Units," Journal of Intelligent Information Management, Vol. 2, pp. 306-315, 2010.
8. Seong, K. H., Cho, H. W., Hwang, J. H. and Shim, J. Y., "Power Loss and Thermal Characteristic Analysis of Induction Motors for Machine Tool Spindle according to the Rated Power-Speed," The Transactions of the Korean Institute of Electrical Engineers Vol. 62, No. 12, pp. 1668-1677, 2013.
9. Choi, H. J., and Choi, S. D., "Thermal Characteristics Analysis of High Speed Spindle of CA Frame Equipment for Eyewear," Journal of the Korean Society of Manufacturing Process Engineers, Vol. 10, No. 5, pp. 31-37, 2011.
10. Dong, Y., Zhou, Z. and Liu, M., "Bearing Preload Optimization for Machine Tool Spindle by the Influencing Multiple Parameters on the Bearing Performance," Journal of Advances in Mechanical Engineering, Vol. 9, No. 2, pp. 1-9, 2017.
11. Kim, S. T., Lee, S. J. and Choi, Y. H., "Thermal Characteristics Analysis of a High Speed Spindle System by Using FSI Method," Jorunal of the Korean Society of Manufacturing Process Engineers, Vol. 13, No. 3, pp. 83-88, 2014.
12. Lee, M. G., Nam, S. H. and Lee, D. Y., "Lightweight of Movable Parts for Energy Reduction of 5-axis Machining Center," Journal of the Korean Society for Precision Engineering, Vol. 30, No. 5, pp. 474-479, 2013.
13. Kwon, S. W., Tong, V. C. and Hong, S. W., "Modeling of Displacement of Linear Roller Bearing Subjected to External Forces Considering LM Block Deformation," Transactions of the Korean Society of Mechanical Engineers A, Vol. 40, No. 12, pp. 1077-1085, 2016.